Journal of the Ceramic Society of Japan 134 [5] 375-382 2026
DOI https://doi.org/10.2109/jcersj2.26016

JCS-Japan

FULL PAPER

Structural color coatings for ceramics and glass surface by silica opal films

Hiroshi Fudouzi[1,†]

[1]National Institute for Materials Science, 1–2–1 Sengen, Tsukuba, Ibaraki 305–0047, Japan

Structural colors derived from colloidal crystals are gaining attention as new color materials that are non-toxic and minimize environmental pollution. Vivid structural colors were formed by coating glass and ceramics with a colloidal crystal (opal) thin film composed of silica particles. This paper focuses on reporting this thin film formation process. A milky-white suspension of silica particles (particle size 290 nm) precisely arranged on the substrate surface exhibited vivid red structural color after drying. The dip coating is not limited to flat substrates like glazed ceramics or glass; it is versatile and can be applied to curved surfaces, uneven surfaces, and even rough, unglazed ceramic surfaces. Optical evaluation utilized reflectance spectra. By employing silica opal films with varying particle sizes, diverse colors spanning the entire visible spectrum from blue to red were achieved. Furthermore, through heat treatment and modification to create a hydrophobic surface, stable structural color emission was enabled, preventing loss of color due to abrasion or wetting.

Key-words : Silica colloid, Colloidal crystal, Structural color, Opal film, Bragg's diffraction, Hydrophobic, Glaze

[Received February 16, 2026; Accepted March 6, 2026; Published online April 2, 2026]

1. Introduction

Structural color is a widely observed phenomenon in nature and living organisms.[1] Rather than originating from pigments or dyes, this coloration comes from nanostructures. Humans have valued structural color in jewelry and other valuable materials since ancient times. Examples of structural color in nature include a jewel beetle, a peacock's feather, the pearl and opal. In contrast, examples of artificial structural colors in glass and ceramics include ancient Roman iridescent glass[2] and Tenmoku tea bowls.[3] These artifacts are also captivated modern people with their unique hues of structural color, which are distinct from pigment-based colors. In recent years, research on structural color materials using biomimetic approaches has been actively pursued.[4] Additionally, research on structural color and optical sensors using multilayer films of one-dimensional photonic crystals via liquid-phase processes has flourished.[5–7] The main materials used are organic polymers and soft materials. However, a high refractive index is necessary for excellent photonic properties. Thus, for example, studies have investigated forming multilayer films of inorganic substances via liquid-phase processes.[8] One of important advantages of structural colors is that they avoid harmful pigment components, making them promising as safe, environmentally friendly color materials from an engineering perspective.

Silica particle aggregates exist in two types (amorphous and colloidal crystals), each exhibiting distinct structural color characteristics. P. Chi et al. reported the creation of colored glazes featuring amorphous photonic crystal structures that exhibit diverse coloration without any coloring agents.[9] Research on structural colors, including the synthesis of glazes mimicking tenmoku glaze and the elucidation of their coloration mechanisms, has attracted significant attention. Amorphous photonic crystal structural color glazes,[10,11] which exhibit non-iridescent color independent of viewing angle, are sensitive to firing conditions due to their phase-separated structure with short-range order. These are structural colors originating from amorphous photonic crystal structures.[12,13] In contrast, the latter exhibits angle-dependent structural colors due to Bragg diffraction of visible light by colloidal crystals.[14,15] This structural color mechanism originates from photonic crystal function by three-dimensional colloidal crystal arrays (opal or inverse opal structures).

This type of structural color of inorganic colloidal crystals also has been potential applications for a structural color coating in ceramics or glass wares. For the pioneer works for alternative pigments, A. Stein et al. reported in the field of research using harmless, low-environmental impact zirconium oxide as a pigment substitute to achieve structural colors with colloidal crystals.[16] They fabricated inverse opal structures of zirconia using colloidal crystals composed of polymer colloidal particles as templates. By selecting the particle size of the polymer particles, the researchers reported success in producing powder pigments ranging from purple to red.[17] Subsequent reports indicated the existence of structural color pigments using

---

[†] Corresponding author: H. Fudouzi; E-mail: FUDOUZI.Hiroshi@nims.go.jp

silica instead of ZrO_2. By strategically manipulating the periodicity of the granular inverse opal's porous structure, the development of three monochromatic pigments; red, green, and blue was achieved. Mixing these pigments enabled the creation of mixed-color pigments such as cyan (blue and green combination), yellow (green and red combination), and magenta (red and blue combination).

Colloidal suspension as an ink for structural color coating are anticipated wide field industrial color decorations. For example, coating a car shape surface,[18] coating silica colloids on conductive surface by electrophoresis deposition.[19] Beyond interior decoration, the structural color of opal is expected to find applications in automotive exterior coatings and interior finishes. In recent the core challenge in structural color applications lies in the formulation of colloidal inks or paint suspensions. As alternative pigment materials, numerous research groups[20–23] are advancing studies on polymer or silica colloidal suspensions as novel colored, non-toxic, environmentally friendly pigments or dyes.

The academic research on color decoration for glass and ceramics is scarce. As one of the few examples, Fukazawa et al.[24] attempted to apply colloidal crystals as structural color ink onto ceramics and glass. They used alkoxide silicon as monodisperse colloidal particles, incorporated polymer as an additive, and adopted a water-alcohol solution as the ink solvent. This ink was applied with a brush to form patterns on ceramic and glass containers. Ultimately, thermal treatment at 500 °C burned off the polymer, forming a porous periodic structure that exhibits structural color. Although not explicitly stated in the paper, it is presumed that a silica inverse opal structure was formed. Recently, Ono reported on the formation of structural color by coating silica particle suspensions onto ceramic and glass container surfaces.[25] To fix the silica opals arranged for practical applications, silicon alkoxide was added as a precursor to the suspension ink and fixed via heat treatment. This ink is easy to use in the conventional ceramic process. In a different approach, Kohoutek et al. formed a single-particle film of silica colloids using the Langmuir–Blodgett method and transferred it onto a glass sphere surface.[26] Decorative applications on glass spheres are anticipated to utilize structural color as an interior design element.

This paper proposes a simple and convenient technique for imparting structural color to surfaces in glass and ceramic. This technique deposits opal thin films onto target surfaces via a liquid-phase process originating from a monodisperse silica colloid suspension. A dip-coating method using polystyrene particles has already been developed for biomimetic research on novel structural color materials.[27] This study focuses on silica particles, aiming to establish a practical process for imparting structural color to glass and ceramics. As competing technologies, engineering techniques for dry processes to impart structural color to ceramic and glass surfaces are well-established. For example, one method involves multilayer coating via Physical Vapor Deposition (PVD) under vacuum conditions.[28,29] This technology is a color decoration technique derived from dielectric mirror manufacturing. Compared to these existing dry coating processes, the proposed wet coating process holds potential for reducing large manufacturing costs since it does not require expensive vacuum coating equipment.

2. Experimental section

2.1 Chemical & materials

Silica colloid suspensions (Silbol EX series, Diameter size from 210 to 310 nm dispersed in water, 30 wt % concentration) were obtained from Fuji Chem., Co. (Osaka, Japan). The other chemicals purchased from as follows and use in no purification. Ethanol (99.5 %, Kishida Chemical Co., Ltd., Osaka, Japan), polydimethylsiloxane, PDMS fluid (KF-96, 100cs, Shin-Etsu Chemical Co., Ltd., Tokyo, Japan) and Hexane and Isopropanol (Kanto Chemical, Inc., Tokyo, Japan). Silica opal thin films were applied to a black glass plate (Shade #13 filter plate, 55 mm × 110 mm, $t = 3$ mm) obtained from Trusco Nakayama Co., Tokyo, Japan. Small black ceramic and tile products (obtained from Kusaba Chemical Co., Ltd., Tajimi, Japan), either unglazed or with a glaze layer, were used as test pieces for the coating experiment.

2.2 Coating procedure

As illustrated in **Fig. 1**, the process is comprised of three steps, coating opal film, heat fixing deposited silicas and surface modification. The dip coating targets is slowly withdrawing from a suspension of silica colloidal particles dispersed in an ethanol aqueous solution. The dip coaters (Homemade equipment using an actuator with stepping motor) are shown in supplementary Fig. S1. The suspension was prepared by diluting a silica particle suspension dispersed in water with ethanol at a 1:3 weight ratio. The suspension concentration was approximately 7.5 wt %. The substrate lifting speed was extremely slow, approximately from 0.1 to 0.6 µm/s. The suspension formed a liquid film on the substrate surface and, during evaporation, self-assembled into a densely packed colloidal crystal (opal) thin film. This lifted silica opal was merely deposited, and its arrangement could be easily disrupted by scratching or similar actions. Therefore, it was fixed by heat treatment in an electric furnace (FO511, Yamato Scientific Co., Ltd., Tokyo, Japan). The heat treatment temperature varied depending on the substrate: 1000 °C for 5 h for ceramic substrates and 400 °C for 5 h for black glass plates. Subsequently, to prevent structural color changes caused by water infilling among silica particles in the opal film, the silica opal surface was modified water repellency has been imparted by a bake-on method described in the technical note.[30] A coating liquid composed of PDMS fluid, dissolved in hexane, was diluted to a specific percentage at 4.8 wt.%, and the substrate was drawn off at a controlled velocity of 0.4 millimeters per second. The top surface was modified to a hydrophobic state through a heat treatment process at 300 °C for a duration of 5 min. Additionally, to remove any excess PDMS liquid remaining on

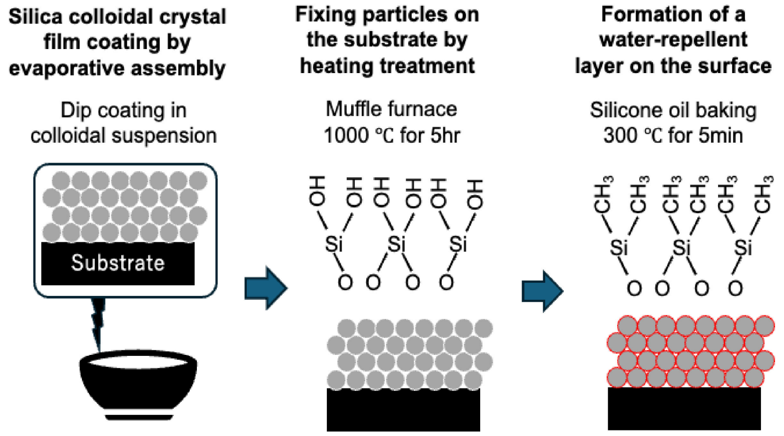

Fig. 1. A conceptual procedure for stable structural color of silica colloidal crystal (opal) films on ceramic or glass surfaces. Heat treatment improved bonding silica colloids to the substrate without loss of structural color and, hydrophobic modification to protect change or lost structural color by wetting water on the surface.

the opal film, the substrate was cleaned with isopropanol. The opal film surface characteristics changed from hydrophilic to hydrophobic as the surface of the silanol group was substituted with a methyl group as illustrated in Fig. 1. This treatment keeps the structural color from water wetting.

2.3 Characteristic evaluation

Digital camera (EXILIM EX-F1, CASIO Computer Co., Ltd., Tokyo, Japan). Reflection photo image and movie were obtained under using a flat high brightness LED white light (Color temperature: 5000 K, Shinkosha Co., Tokyo, Japan) uniform irradiation. To minimize the influence of angle dependence in structural color, photographs were taken using a homemade coaxial illumination system (As supplementary shown in Fig. S2). The microstructure of the colloidal photonic crystal films was observed using a Scanning Electron Microscope, SEM (JSM-6500F, JEOL Ltd., Tokyo, Japan).

The reflectance spectra of the silica opal films were recorded using a miniature fiber optic spectrometer (Ocean Optics, USB2000+, Dunedin, FL, USA). The incident light was perpendicular to the samples (to measure specular reflectance, the probe was oriented at 90° to the sample in a reflectance probe holder) at a local spot (less than 2 mm in diameter) by HL-2000 tungsten halogen light source. The fiber has a core diameter of 200 µm, a numerical aperture of 0.22, and is banded with six illumination fibers around a single read fiber.

The fixing effect of heat treatment on silica opal is evaluated by assessing its wear resistance using a cotton swab subjected to a load and moved horizontally back and forth. A simple reciprocating wear tester (MMS-1, AS ONE Co., Tokyo, Japan) was used to the glass plate.

Surface hydrophilic and hydrophobic property was evaluated by the contact angle of a drop of pure water. A contact angle meter (Simage Standard 100, 1.5M pixel CCD camera, Excimer Inc., Yokohama, Japan) was used and analysis by a half-angle method. Assuming the shape of the drop of water dropped on the sample is a perfect circle, the contact angle can be found from the radius and height of the circle. Here we obtained the contact angle as calculated by finding the angle of the line connecting the left and right endpoints of the drop to the vertex, relative to the solid surface, and doubling this as described later.

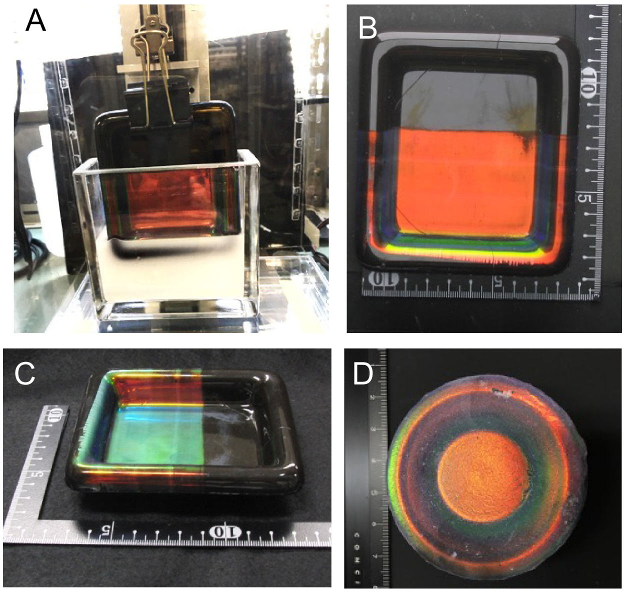

Fig. 2. A process for forming a red structural color film on a black ceramic plate by coating at a slow speed from a colloidal silica suspension. The silica with 290 nm diameter solution showed white milky color and the opal film showed red structural color.

3. Results and discussion

3.1 Opal films coating on ceramic test pieces

As illustrated in **Fig. 2**, silica particles with a diameter of 290 nm were coated onto the surfaces of commercially available ceramic products, thereby producing a red structural color. In Fig. 2(A), the photo shows a glazed square plate being elevated at a very low speed from a silica suspension. When photographed with coaxial illumination from directly above, a red structural color is observed

[Fig. 2(B)]. Conversely, when observed from a tilting perspective, the structural color transitions to green, as illustrated in Fig. 2(C). This angle dependence of the structural color is a phenomenon common to colloidal crystals (opal thin films). In Fig. 2(D), silica opal was applied to the surface of an unglazed, unfinished round plate. The surface is uneven and not flat, however a red structural color is observed. When viewed at tilting angle, the structural color changed to green. The red structural color exhibited is influenced by particle concentration and lifting speed. The coating film exhibits a change in its structural color from a pale red state to an opaque state as it transitions from a thin to a thick state. Additionally, the presence of thick coating films was observed to undergo a process of peeling and detachment from the ceramic surface. The most suitable coating conditions were estimated to be a particle concentration of approximately 10 wt% and a withdraw speed ranging from 0.1 to 0.6 µm/s.

One of the issues in this suspension process is the extremely slow the withdraw speed for applied to engineering use. The authors have previously reported a faster coating process in their existing research.[31] We have demonstrated that increasing the particle concentration of the suspension by one order of magnitude enables colloidal crystals to form films in a short time. However, in this study, priority was given to the crystallinity of the colloidal crystals, so accelerating the film formation speed remains a future challenge.

Another challenge in silica opal film coating is the unintended formation of colloidal crystal lines perpendicular to the substrate during substrate lift-off from the silica suspension. As the mechanism behind this phenomenon remains unclear, this paper presents it as a technical issue to be resolved in Fig. S3 as the supplementary information. This tendency to form silica aggregated lines were observed not across the entire substrate but specifically at the start of withdraw. Even under identical deposition conditions, locally formed lines are sometimes observed while others are not. It is highly probable that silica particle aggregates in the suspension adhere to the substrate and serve as growth nucleation sites. Future work in production must clarify the cause of this phenomenon and establish suppression methods.

3.2 Structural color design by silica size

The structural color of silica opal is contingent upon the particle size of its constituent colloidal particles. **Figure 3** shows the structural colors observed on the black glass plate as the particle size (diameter) was varied from 210 to 310 nanometers by 10 nm steps. The structural colors exhibited a wide spectrum, ranging from blue to red. The coloration of silica colloidal crystals is attributable to Bragg's diffraction in visible wavelength spectrum color. From a theory, it is well known that the structural colors of colloidal crystals depend on the particle size. One peak of Bragg's diffraction (appearing from 400 to 700 nm) causes structural color in the visible wavelengths below. Here λ is diffraction peak position, d_{111} is an interspace of cubic closely packing (ccp) layers and n_{eff} is average refractive index as expressed in Eq. (1).[14] In addition, θ, D, n_{p}, n_{m}, V_{p}, V_{m} are corresponding to incident angle, silica particle diameter, refractive index of silica, refractive index of air, volume of particle, volume of air, respectively.

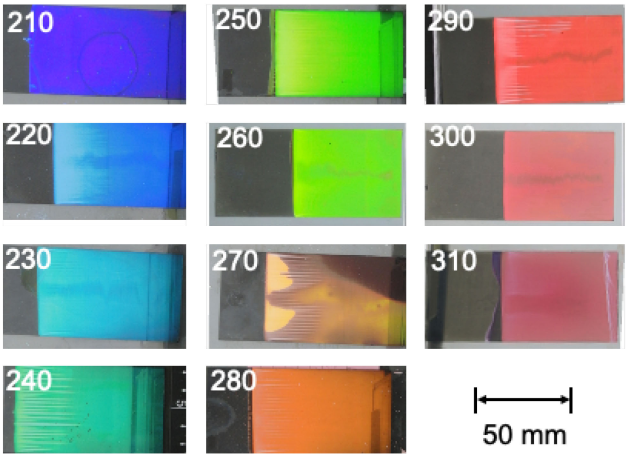

Fig. 3. Diverse spectrum types of structural colors exhibited by thin films of colloidal crystals composed of silica particles with varying diameters on black glass plates. The white numbers indicate the diameter of the silica colloids (in nm).

$$\lambda = 2d_{111}\sqrt{(n_{\mathrm{eff}}^2 - \sin^2\theta)} \tag{1}$$

$$d_{111} = \sqrt{\frac{2}{3}}D \tag{2}$$

$$n_{\mathrm{eff}}^2 = n_{\mathrm{p}}^2 V_{\mathrm{p}} + n_{\mathrm{m}}^2 V_{\mathrm{m}} = 0.74n_{\mathrm{p}}^2 + 0.26n_{\mathrm{m}}^2 \tag{3}$$

Here $\theta = 0$, $n_{\mathrm{p}} = 1.4$ and $n_{\mathrm{m}} = 1$. From Eqs. (1), (2) and (3), we obtain following a relationship between the peak position (wavelength) and the silica particle size (diameter). The reflection peak wavelength, as calculated theoretically, is expressed in Eq. (4).

$$\lambda = 2.136D \tag{4}$$

Figure 4 shows the superimposed reflection spectra of the three structural colors (blue, green, and red). Within the visible light range of from 350 to 750 nm, one large reflection peak and several smaller peaks (called fringes) are observed for each color. The fringes result from thin-film interference and cause structural coloration. However, their intensity is lower compared to the Bragg diffraction peak. Therefore, the primary structural color visible can be described as a nearly monochromatic color originating from the single, intense Bragg diffraction reflection peak. The particle sizes were 210 nm for blue silica particles, 250 nm for green, and 290 nm for red. The difference in particle size required to generate the three structural colors was only 40 nm. As shown in Eq. (4), a positive correlation exists between particle size and the peak wavelength of Bragg diffraction. Therefore, the relationship between particle size and peak wavelength was measured for the structural colors shown in Fig. 3.

Figure 5 demonstrates the relationship between structural color and reflection peaks wavelength for particles of

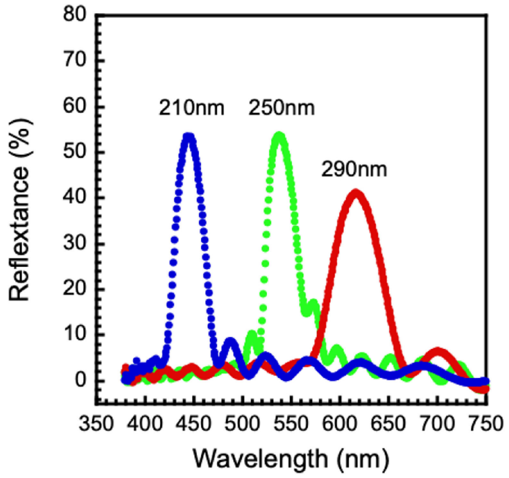

Fig. 4. Structural colors with different particle sizes and their reflection spectra. Reflection spectra for silica particles at sizes of 210, 250, and 290 nm.

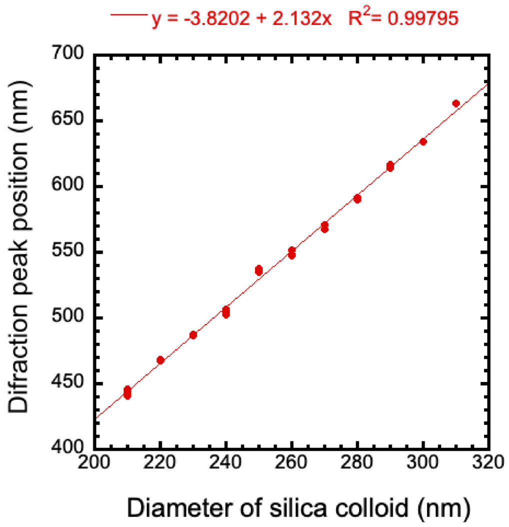

Fig. 5. Relationship between silica particle size and Bragg's diffraction peak wavelength. Red circles are data and the red straight line indicates a linear approximation using least squares cut.

various sizes, as illustrated in Fig. 3. The slope of the line is 2.132 and R^2 is 0.998. The measurement results demonstrated a high correlation between particle size and the observed wavelength, yielding results that closely approximated the calculated value of 2.136 derived from the Bragg equation with Snell's law [Eq. (4)]. As illustrated in Fig. 5, the graph encompasses a substantial portion of the visible spectrum region between 440 and 660 nm. These results demonstrate that structural colors can be produced in diverse hues solely by only selecting the particle size of silica particles.

3.3 Heating opal film on ceramics and black glass

Simply forming silica opal results only in the deposition of silica particles on the ceramic surface. These deposited particles can be easily scraped off the surface with light scratching. Therefore, fixing the particles is critically important from an engineering perspective. One effective method for this is a fixation process using heat treatment (the second stage shown in Fig. 1). **Figure 6** shows the result of heat treating the silica opal film on a glazed tile test specimen at 1000 °C for 5 h. A slight color change was observed before and after heating, with the structural color shifting slightly from red to orange [Fig. 6(A)]. This change in structural color can also be confirmed by comparing the reflectance spectra before and after heating. The heat treatment caused a peak shift (8.3 nm) toward the lower wavelength side. From the Eq. (1), d_{111} (the interlayer spacing in the ccp layer of the silica opal film) likely decreased due to thermal shrinkage. The optimization of heat treatment conditions is imperative for effective particle fixation. Furthermore, Figs. 6(C) and 6(D) show SEM images of the microstructure of the silica opal film surface after heat treatment. The (111) planes of the CCP structure maintained their orientation even after heat treatment.

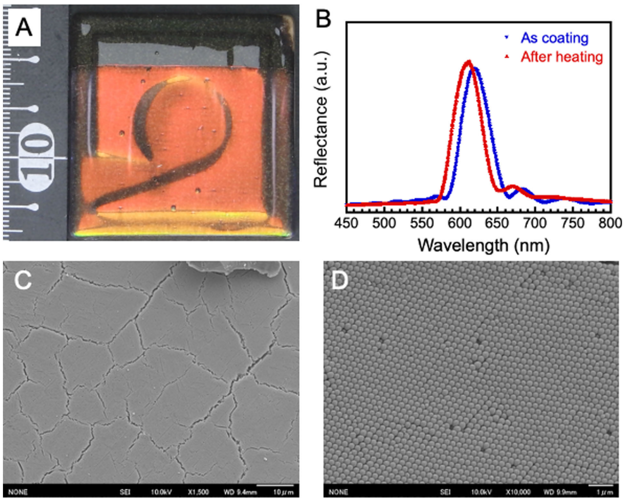

Fig. 6. Heat treatment for fixing silica particles. A) Photo after heating, B) Reflectance spectrum before and after heating treatment, C) and D) SEM images microstructures of surface of the silica opal of 290 nm film after heating.

The efficacy of the heat treatment process in adhering silica opal film to the substrate can be determined through the implementation of an abrasion test. Due to constraints imposed by the equipment, it was not possible to conduct abrasion testing in this instance for the ceramic plate [Fig. 6(A)]. However, a rudimentary evaluation revealed no occurrence of silica particle detachment, even under manual manipulation with a finger. The quantitative evaluation of abrasion resistance remains a future task. In contrast, the thermal treatment effect on silica opal film on a flat glass plate was evaluated by a simple reciprocating wear tester shown in **Fig. 7**. The force applied to the cotton rod was 0.98 N, with a reciprocating speed of 33 rpm and a stroke of 22 mm. Test specimen B, which was silica opal without heat treatment, showed silica particles peeling off after one cotton swab reciprocation, exposing the underlying glass substrate. Specimens C, D, and E correspond to heat treatment conditions of 350 °C for 5 h,

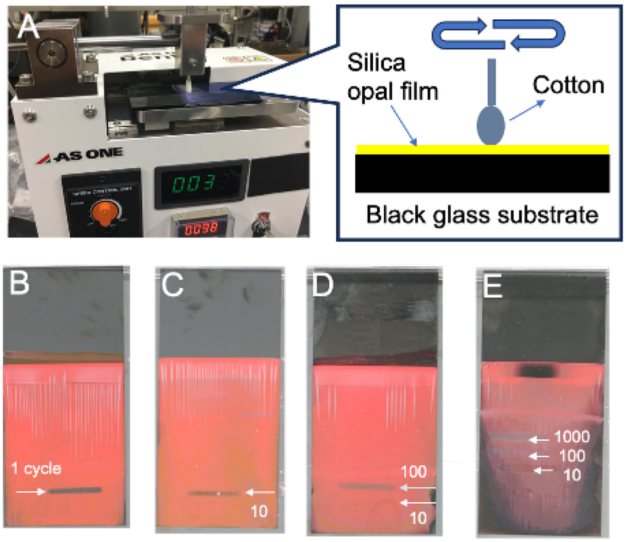

Fig. 7. Wear resistance evaluation for silica opal film on black glass after heating. A) a simple reciprocating wear tester. Scratch marks caused by a cotton swab, B) No heating, C) 350 °C-5 h, D) 400 °C-5 h and E) 450 °C-5 h.

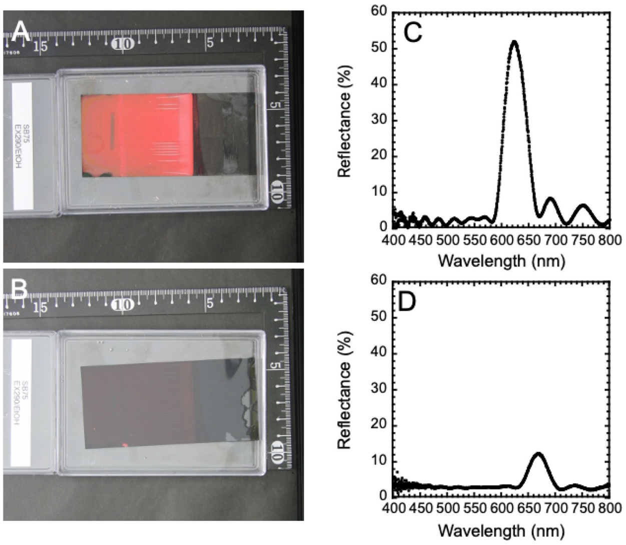

Fig. 8. The phenomenon of reversible structural color changes, precipitated by pure water wetting of silica opal film (after heating 400 °C-5 h). A) Red structural color (Dry film condition) and B) Almost colorless (Wet film condition). The reflectance spectra C and D correspond to the photos A and B, respectively.

400 °C for 5 h, and 450 °C for 5 h, respectively. Test specimen C exhibited scratches exposing the substrate after 10 cycles. The specimens D and E showed improved wear resistance. Specimen D exhibited weak scratches after 100 cycles. Specimen E, however, exhibited scratches after 1000 cycles. It was found that the fixation strength of silica particles increases with rising heat treatment temperature. However, heat treatment at 450 °C caused partial loss of the structural color of silica opal. This relates to the heat resistance of the glass substrate and indicates an upper limit to the heat treatment temperature. For the black glass substrates used in this experiment, heat treatment at 400 °C for 5 h was concluded to be the optimal condition balancing both wear resistance and structural color retention.

3.4 Surface modifications

Another challenge with the structural color of silica opal is the phenomenon where the structural color disappears when the surface is wetted with water shown in **Fig. 8**. The silica opal film, composed of 290 nm silica particles following heat treatment (400 °C for 5 h), exhibits a red structural color Fig. 8(A). The structural color of the film is known to disappear upon its wetting by water, shown in Fig. 8(B). However, upon drying, the original red structural color recovers, as original condition. The observed phenomena are believed to originate from Bragg diffraction peaks in the reflection spectrum Figs. 8(C) and 8(D), respectively. In dry condition, the diffraction peak was 624 nm and its reflectance was 51.8 %. In addition, many small peaks due to fringe. In contrast, in wet condition, the diffraction peak shifted to 668.1 nm (near NIR wavelength) and the reflectance was 12.2 %. This peak shift and reducing intensity origin colorless of silica opal film. When the silica opal was exposed to water, the peak demonstrated a significant decrease in intensity. Following the evaporation of the liquid film and subsequent drying, the reflection peak underwent a recovery to its initial state.

The disappearance of structural color is thought to be primarily caused by the transition of the interstitial space in silica opals from air (1.00) to water (1.33). Consequently, the average refractive index in Eq. (3) increases from 1.308 to 1.375. The peak shift calculated from Eq. (4) based on the peak shift amount was 31.6 nm. Although slightly smaller than the measured value (43.7 nm), main reason can be qualitatively explained by water molecules filling the gaps between silica particles, shifting the peak from the visible (red) to the near-NIR region, a quantitative explanation for the reducing peak intensity remains unclear. However, Fig. 8 suggested that preventing wetting can serve as one countermeasure to achieve the disappearance of structural color. Inspired by the knowledge of technical note,[30] a water-repellent layer was formed on the surface of the silica opal (corresponding to the third step in Fig. 1).

Figure 9 shows the contact angle measurements are contingent upon the surface condition of silica opal. The hydrophobic treatment described in this paper was carried out using the bake-method outlined in the technical notes of the silicone oil manufacturer. Figures 9(A), 9(B) and 9(C) are Photos taken from directly above to measure contact angles on surfaces with different surface conditions. Figure 9(D) shows the contact angle measurement setup. The contact angle was calculated from the measured values obtained from this photograph using Eq. (5). Here θ_c is contact angle of a drop of pure water on silica opal film. h, r are high and radius of water drop shown in Fig. 8(D).

$$\theta_c = 2 \arctan h/r \tag{5}$$

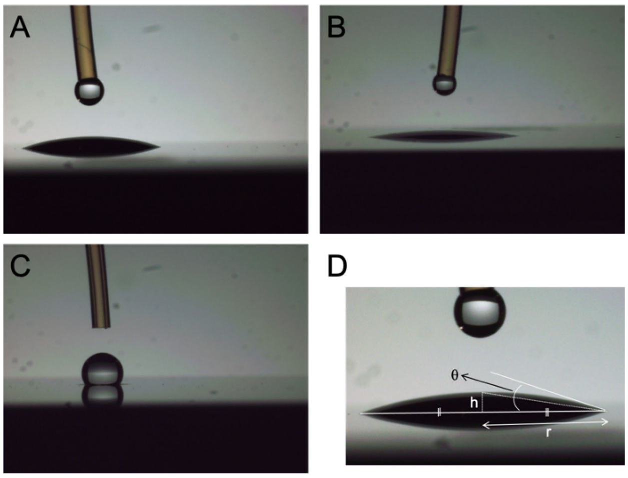

Fig. 9. Changes of contact angles by surface change. A) A drop of water on 250 nm silica opal film, B) After heating the opal film, C) A drop of water formed on a hydrophobic surface. A contact angle was obtained by a half-angle method as shown in D).

Table 1. Silica opal films with different treatments

	Surface conditions of silica opal films	Contact angle, θ_c
A	As coated silica opal film	19.3°
B	After heating, 400 °C for 5 h	11.1°
C	Hydrophobic, 300 °C for 5 min	123.1°

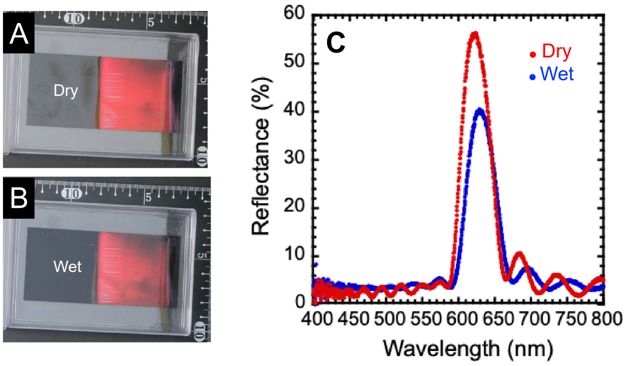

Fig. 10. The hydrophobic silica opal surface effect on structural color of silica opal films. A) Photography on dry condition, B) Photography on wet condition, and C) Spectrum comparison of dry and wet conditions.

The contact angles for the three surface states shown in Fig. 1 were summarized in **Table 1**. Here silica opal consists of 250 nm in diameter. In case of C, the contact angles indicate over 100 degrees. According to the technical note,30) the silica surface suggested modified from a hydrophilic surface due to silanol groups to a highly hydrophobic surface with methyl groups substituted.

Figure 10 shows the water-repellent effect of the hydrophobic surface of silica opal in pure water. The test specimen was prepared by depositing a 290 nm diameter film on a black glass substrate, fixing it by heat treatment at 400 °C for 5 h, and then treating the silica particle surface with a hydrophobic coating using the silicon oil baking method.30) Figure 10(A) shows the silica opal in its initial state exhibiting a red structural color when dry. Figure 10(B), on the other hand, shows the substrate immersed in pure water. No significant color change is observed. Figure 10(C) compares the reflection spectra in the dry and wet states. The peak wavelength shifted 6.7 nm toward the longer wavelength side during the transition from the dry to the wet state. Conversely, the peak intensity decreased by 15.8 % due to wetting. Comparing these results with the hydrophilic surface in Fig. 8(D) clearly demonstrates the surface modification effect. Hydrophobic treatment of the silica opal layer is effective in suppressing the disappearance of structural color caused by water. Regarding the baking process of silicone oil that replaces silanol groups on the surface of silica opal with methyl groups, further detailed investigation, including its mechanism, is necessary.

4. Conclusion

The color decorating process by dip coating from a silica colloid with uniform particle size suspension to form colloidal crystal films. The result with high quality colloidal crystal is silica opal film with vivid structural color due to Bragg's diffraction. The following substrates were coated: black glass plates, unglazed and glazed ceramic dishes, and black tile with glaze. The opal film coating's versatility extends beyond flat and smooth surfaces, as it can also be applied to curved surfaces and even the uneven surfaces of unglazed ceramics.

Additionally, it was determined that the structural colors can be selected by altering the size of the silica particles. This study confirmed that the optical properties of the color-producing layer can be controlled using silica particles, enabling color control of the spectrum from blue (particle size 210 nm) to red (particle size 310 nm).

Finally, to stabilize the arranged silica opal films, particle fixation was achieved through a thermal treatment process, and the surface layer was rendered hydrophobic to prevent structural color loss due to wetting. This demonstrated the potential to form stable structural color films on ceramic and glass substrates. These results indicate the possibility of replacing existing pigments that are harmful or have significant environmental impacts.

Acknowledgements The author thanks Ms. Kaori Terui for her technical support on experiments. This work has been financially supported by the Okura Kazuchika Memorial Foundation in 2024 Research Grant. The ceramic products were obtained from Kusaba Chemical Co., Ltd., Tajimi, Japan. In addition, a part of this work (Taking SEM image photos by JSM-6500F) was supported by the "Advanced Research Infrastructure for Materials and Nanotechnology in Japan (ARIM)" of the Ministry of Education, Culture, Sports, Science and Technology (MEXT). Proposal Number JPMXP1225NM5378.

References

1) S. Kinoshita and S. Yoshioka, in "Structural Colors in Biological Systems", Ed. by S. Kinoshita and S.

Yoshioka, Osaka University Press (2005) pp. 3–26.
2) G. Guidetti, R. Zanini, G. Franceschin, M. Moglianetti, T. Kim, N. Cohan, L. Chan, J. Treadgold, A. Traviglia and F. G. Omenetto, *P. Natl. Acad. Sci. USA* 120, e2311583120 (2023).
3) C. Y. Chiang, H. F. Greer, R. Liu and W. Zhou, *Ceram. Int.* 42, 7506 (2016).
4) A. Saito, *Sci. Technol. Adv. Mat.* 12, 064709 (2011).
5) Y. Qi and S. Zhang, Structural color due to self-assembly, in "Functional Materials from Colloidal Self-Assembly", Ed. by G. Zhao and Q. Yan, Wiley-VCH GmbH (2022) pp. 183–235.
6) E. Palo, M. A. Papachatzakis, A. Abdelmagid, H. Qureshi, M. Kumar, M. Salomäki and K. S. Daskalakis, *J. Phys. Chem. C* 127, 14255 (2023).
7) W. Feng, J. Paika and L. J. Guo, *Mater. Chem. Front.* 8, 3474 (2024).
8) T. Yasuda and T. Takeuchi, *J. Ceram. Soc. Jpn.* 131, 330 (2023).
9) J. Zhu, P. Shi, F. Wang, L. Dong and T. Zhao, *J. Ceram. Soc. Jpn.* 124, 229 (2016).
10) P. Shi, F. Wang, J. Zhu, H. Yang, Y. Wang, Y. Fang, B. Zhang and J. Wang, *J. Eur. Ceram. Soc.* 38, 2228 (2018).
11) B. Zhang, Y. Wu, Z. Jin, H. Ning, F. Wang, H. Luo, J. Zhu, C. Yang and P. Shi, *J. Ceram. Soc. Jpn.* 132, 438 (2024).
12) Y. Takeoka, *J. Mater. Chem.* 22, 23299 (2012).
13) G. Topçu, T. Güner and M. M. Demir, *Photonic. Nanostruct.* 29, 22 (2018).
14) H. Fudouzi, *J. Colloid Interf. Sci.* 275, 277 (2004).
15) H. Fudouzi, *Adv. Powder Technol.* 20, 502 (2009).
16) R. C. Schroden, M. Al-Daous, C. F. Blanford and A. Stein, *Chem. Mater.* 14, 3305 (2002).
17) D. P. Josephson, M. Miller and A. Stein, *Z. Anorg. Allg. Chem.* 640, 655 (2014).
18) M. Ishii, *R&D Review of Toyota CRDL* 45, 17 (2014).
19) K. Katagiri, Y. Tanaka, K. Uemura, K. Inumaru, T. Seki and Y. Takeoka, *NPG Asia Mater.* 9, e355 (2017).
20) M. Iwata, M. Teshima, T. Seki, S. Yoshioka and Y. Takeoka, *Adv. Mater.* 29, 1605050 (2017).
21) M. Kohri, *Sci. Technol. Adv. Mat.* 21, 833 (2020).
22) C. Park, K. Koh and U. Jeong, *Sci. Rep.-UK* 5, 8340 (2015).
23) R. Ohnuki, M. Sakai, Y. Takeoka and S. Yohioka, *Langmuir* 36, 5579 (2020).
24) N. Fukazawa and R. Jin, *Hyoumen Gijutsu* 61, 754 (2010) [in Japanese].
25) Y. Ono, *J. Asian Ceram. Soc.* 8, 578 (2020).
26) T. Kohoutek, M. Parchine, M. Bardosova and M. E. Pemble, *Colloid. Surface. A* 593, 124625 (2020).
27) H. Fudouzi and T. Hariyama, *J. Jpn. Soc. Colour Mater.* 93, 149 (2020) [in Japanese].
28) M. Vorobyova, F. Biffoli, W. Giurlani, S. M. Martinuzzi, M. Linser, A. Caneschi and M. Innocenti, *Materials* 16, 4919 (2023).
29) S. Niyomsoan, W. Grant, D. L. Olson and B. Mishra, *Thin Solid Films* 415, 187 (2002).
30) Technical data sheets, Silicone fluids KF-96 performance test results, Shin-Etsu Chemical Co., Ltd, https://www.shinetsusilicone-global.com/catalog/pdf/kf96_e.pdf (2014).
31) G. T. H. Tran, M. Koike, T. Uchikoshi and H. Fudouzi, *Langmuir* 36, 10683 (2020).